Alginate bone scaffolds coated with a bioactive lactose modified chitosan for human dental pulp stem cells proliferation and differentiation

Davide Porrelli [a,*], Martina Gruppuso [a], Federica Vecchies [b], Eleonora Marsich [c], Gianluca Turco [a]

[a] Department of Medicine, Surgery and Health Sciences, University of Trieste, Piazza dell'Ospitale 1, 34125 Trieste, Italy
[b] Department of Life Sciences, University of Trieste, Via Licio Giorgieri 5, 34127 Trieste, Italy
[c] Department of Medicine, Surgery and Health Sciences, University of Trieste, Via Licio Giorgieri 5, 34129 Trieste, Italy

ARTICLE INFO

Keywords:
Scaffolds
Alginate
Bioactive lactose-modified chitosan
Human dental pulp stem cells
Bioactive polysaccharides
Bone regeneration

ABSTRACT

Bioactive and biodegradable porous scaffolds can hasten the healing of bone defects; moreover, patient stem cells seeded onto scaffolds can enhance the osteoinductive and osteoconductive properties of these biomaterials. In this work, porous alginate/hydroxyapatite scaffolds were functionalized with a bioactive coating of a lactose-modified chitosan (CTL). The highly interconnected porous structure of the scaffold was homogeneously coated with CTL. The scaffolds showed remarkable stability up to 60 days of aging. Human Dental Pulp Stem Cells (hDPSCs) cultured in the presence of CTL diluted in culture medium, showed a slight and negligible increase in terms of proliferation rate; on the contrary, an effect on osteogenic differentiation of the cells was observed as a significant increase in alkaline phosphatase activity. hDPSCs showed higher cell adhesion on CTL-coated scaffolds than on uncoated ones. CTL coating did not affect cell proliferation, but stimulated cell differentiation as shown by alkaline phosphatase activity analysis.

1. Introduction

Oral rehabilitation of edentulous patients using endosseous implants is a widely used method that can ensure predictable and reliable long-term outcomes (Albrektsson et al., 2017; Bosshardt et al., 2017). Despite this evidence, unfavorable conditions at the alveolar ridges due to atrophy, periodontal disease, or trauma sequelae may result in insufficient vertical or horizontal bone dimension or an unfavorable intermaxillary relationship, making placement of endosseous or external implants impossible or compromising the esthetic-functional outcome of the prosthetic implant. The use of a graft material to guide physiological bone regeneration is one of the commonly used methods to solve the problem of bone deficit in the jaw (Tettamanti et al., 2017; Zhao et al., 2021). Graft materials can be osteoconductive, i.e., materials that have the function of supporting and scaffolding bone cells, or osteoinductive, which, unlike the previous ones, induce a biological process of differentiation of mesenchymal cells into osteoblastic cells. Currently, autografts, i.e. marrow or cortical portions from the same recipient, are the gold standard procedures. Autogenous bone contains growth factors in its matrix that exert osteoinductive activity, but has several disadvantages involving the risk of donor site morbidity, limited supply, the need for a second surgery, and possible rejection (Fisher et al., 2016; Zhang et al., 2018). To overcome these issues, tissue engineering is a promising approach to address bone regeneration by combining the interaction between osteoconductive and osteoinductive scaffolds and stem cells. A scaffold must be biocompatible, accommodate cells, promote their adhesion and proliferation through its porous structure, and degrade after the formation of the new tissue (Amini et al., 2012; Bouet et al., 2015; Henkel et al., 2013). Moreover, it must be easy to handle, shape and adapt to the cavity while sustaining the mechanical stresses and providing structural support (Roseti et al., 2017). Nowadays, different techniques are used to produce these 3D matrices, which have different shapes and chemical compositions (Fradique et al., 2016). Among the techniques available for scaffold preparation, freeze-drying,

Abbreviations: ALP, alkaline phosphatase; BMSCs, bone marrow stromal cells; CTL, lactose-modified chitosan; CTL-sc, alginate/hydroxyapatite scaffolds coated with CTL; Ctrl-sc, alginate/hydroxyapatite scaffolds; DS, differentiation stimuli; hDPSCs, human dental pulp stem cells; MSCs, mesenchymal stem cells; SBF, Simulated Body Fluid.

* Corresponding author.
E-mail addresses: dporrelli@units.it (D. Porrelli), martina.gruppuso@phd.units.it (M. Gruppuso), fvecchies@units.it (F. Vecchies), emarsich@units.it (E. Marsich), gturco@units.it (G. Turco).

electrospinning and 3D printing are the most used (Abhinandan et al., 2021; De Santis et al., 2011; Ma et al., 2021) and can be used to prepare scaffolds implemented with functionalities to enhance cell adhesion and differentiation such as drug release, magnetic and mechanical stimulations (Cameraro-Espinosa & Moroni, 2021; Ma et al., 2021; Russo et al., 2020). Natural biopolymers, such as polysaccharides (alginate, chitosan, hyaluronan and collagen, to name a few), are commonly used for scaffolds preparation, because they have a bioactive behavior that can mimic the macromolecular environment of native tissue. Bioactivity and mechanical properties can be enhanced by combining biopolymers with ceramics or carbon nanostructures to form composite materials (Gupta et al., 2013; Karadzic et al., 2015; Wahl & Czernuszka, 2006; Yasmeen et al., 2014), or by chemical modification with bioactive groups that can be recognized by the host cells (Guarino et al., 2015; Hersel et al., 2013; Li et al., 2016). The source of cells is also an important choice for a synergistic effect along with the scaffold. Mesenchymal stem/stromal cells (MSCs) are able to differentiate into the three mesenchymal cell lineages (osteocytes, chondrocytes and adipocytes), and show extensive replication in culture (Bianco & Robey, 2001). Nowadays, new attention is paid to stromal cells derived from human dental pulp. The human Dental Pulp Stem Cells (hDPSCs) are multi-potent stem cells, that are similar properties to bone marrow stromal cells (BMSCs); furthermore they are more readily available and the procedure to obtain them is less invasive (Aghazadeh et al., 2017; Tatullo et al., 2015). hDPSCs have been widely investigated due to their potential to be differentiated into odontoblasts, osteoblasts, chondrocytes, adipocytes and neurons, and because they can represent an autologous source of cells that can be exploited in personalized therapies such as in the treatment of periodontal defects or pulpitis, or in the healing of the post-extraction socket (Aimetti et al., 2018; Barbieri et al., 2018; Meza et al., 2019). The goal of this work is to combine a composite scaffold of alginate, CTL and hydroxyapatite (CTL-sc) with mesenchymal stem cells derived from dental pulp tissue. In detail, the structural and biological properties of alginate/hydroxyapatite (Alg/HAp) scaffolds in presence or absence of CTL, a polysaccharide derived from the functionalization of chitosan backbone with lactose moieties, are studied (D'Amelio et al., 2013). Thanks to its biocompatibility, biodegradability, muco-adhesiveness and antibacterial activity, chitosan is a widely used polysaccharide (Ahsan et al., 2018; Alves & Mano, 2008). It has been observed that the modification of its structure with the addition of lactose moieties at the glucosamine residues leads to an increase in the solubility of chitosan at physiological pH (D'Amelio et al., 2013). Moreover, CTL proved to be bioactive towards chondrocytes, leading to the formation of nodules and stimulating type II collagen and glycosaminoglycan synthesis (Donati et al., 2005). CTL also proved to have biological effects on neuronal progenitors, in particular on their formation, maturation, activity and connection (Medelin et al., 2018). These properties may be related to the presence of a type of carbohydrate - binding protein, called Galectin-1 (Marcon et al., 2005), that presents a carbohydrate recognition domain (CRD), that selectively binds β-galactoside residues (Camby et al., 2006); upon interaction with β-galactoside residues, Galectins are able to induce transmembrane signaling and to activate several biological responses involved in cell growth (Tazhitdinova & Timoshenko, 2020). The hypothesis of a combined role of CTL and Galectin-1 in the differentiation to an osteoblast phenotype is supported by the evidence that Galectin-1 is involved in the differentiation of BMSCs (Andersen et al., 2003) and is expressed in hDPSCs (Akpinar et al., 2014); moreover, it was recently shown that CTL is able to stimulate hDPSCs when is used as a coating for thermosets (Rapino et al., 2019). The present work explores the possibility of using CTL-coated Alg/HAp scaffolds in combination with hDPSCs for bone tissue engineering. The aim of the work is to test whether the scaffold's CTL coating is able to positively affect the behavior of hDPSCs in terms of cell adhesion, proliferation and differentiation to an osteoblastic phenotype.

2. Materials and methods

Sodium alginate samples isolated from *Laminaria hyperborea* were provided by FMC BioPolymer AS (Norway). The (viscosity average) relative molecular mass ("molecular weight", MW) was found to be approximately 120,000 Da as determined by capillary viscosimetry (Vold et al., 2006). The composition of the alginate sample was determined by means of ^{1}H NMR (Grasdalen, 1983; Grasdalen et al., 1979) and resulted to be $F_G = 0.68$, $F_M = 1 - F_G = 0.32$, $F_{GG} = 0.57$, $F_{GM+MG} = 0.22$, $F_{MM} = 0.21$, $N_{G>1} = 14$. F_G and F_M denote the mole fraction of alginate monomers as α-L-guluronic acid (G) and β-D-mannuronic acid (M), respectively, F_{GG} indicates the fraction of G dimers, F_{MM} indicates the fraction of M dimers and F_{GM+MG} indicates the fraction of any mixed sequence of G and M (irrespective of sequence). $N_{G>1}$ is the number-average number ($\bar{n}_n$) of G monomer in homopolymeric sequences having $\bar{n}_n \geq 2$. CTL (lactose-modified chitosan, CAS registry number 85941-43-1) was provided by BiopoLife s.r.l. (Trieste, Italy). The chemical composition of CTL was determined by ^{1}H NMR: fraction of acetylated units (FA) = 0.07, fraction of deacetylated units (FD) = 0.33 and fraction of lactose-modified units (FL) = 0.6. The viscosimetric molecular weight of CTL was estimated to be around 910,000 Da (Furlani et al., 2017). Hydroxyapatite (HAp) powder, fluorescein isothiocyanate (FITC), ascorbic acid ($C_6H_8O_6$), δ-gluconolactone (GDL), in-vitro toxicology assay (Resazurin based, Alamar Blue) TOX-8 kit, *para*-nitro-phenyl-phosphate, and phosphate buffered saline (PBS) were purchased from Merck (Darmstadt, Germany). Trypsin/EDTA solutions, Fetal Bovine Serum (FBS), penicillin streptomycin 100×, L-glutamine 100× and Dulbecco's modified Eagle's medium (DMEM) were purchased from EuroClone (Milan, Italy). CellTiter Aqueous One Solution cell proliferation assay kit (MTS assay) was from Promega (Madison, WI, USA). ELISA kits for human osteocalcin and mouse galectin-1 quantification were purchased from Invitrogen (Waltham, MA, USA). All other chemicals were of analytical grade and were purchased from Merck (Darmstadt, Germany).

2.1. Preparation of alginate/hydroxyapatite scaffolds

Homogeneous calcium alginate hydrogels gels were prepared by blending the alginate solution (final concentration 2% w/V) with hydroxyapatite (HAp) (3% w/V) followed by the addition of GDL (60 mM) (Turco et al., 2009). Polymer solutions were then cured in 24-well tissue culture plates (Sarstedt, Newton, NC, USA), pouring 3.2 mL of solution per well. The hydrogels were stepwise cooled by immersion in a liquid cryostat (circulating bath 28 L, VWR, Radnor, PA, USA). Temperature was decreased stepwise from 20 to −20 °C by 5 °C steps with 30 min intervals for equilibration; the samples were then freeze-dried (with an ALPHA 1–2 LD plus freeze-drier, CHRIST, Osterode am Harz, Germany), for 24 h to obtain porous scaffolds. CTL and fluorescein labelled CTL (CTL-fluo) were adsorbed on scaffold surface by soaking the scaffolds in a 0.2% w/V solution of CTL or CTL-fluo for 4 h. Scaffolds were then washed with deionized water and freeze-dried. Scaffolds without CTL will be indicated as Ctrl-sc, whereas scaffolds with CTL will be indicated as CTL-sc.

2.2. Scanning Electron Microscopy (SEM)

Morphological analyses were performed with a Scanning Electron Microscope Quanta250 (FEI, Oregon, USA), in high vacuum, in secondary electron mode, with 30 kV of tension; the working distance was set in order to obtain suitable magnification. Samples were mounted on aluminum stubs covered with a carbon double-sided tape and subsequently gold sputtered with a Sputter Coater K550X (Emitech, Quorum Technologies Ltd., UK).

2.3. X-ray microcomputed tomography analysis

X-ray microcomputed tomography of samples was obtained by means of a custom-made cone-beam system called TOMOLAB (Mancini et al., 2007). Samples were positioned onto the turn table of the instrument and acquisitions were performed with the following parameters: distance source-sample (F_{OD}), 80 mm; distance source-detector (F_{DD}), 250 mm; magnification, 3.1×; binning, 2 × 2; resolution, 8 μm; tomography dimensions (pixels), 2004 × 1335; slices dimensions (pixels), 1984 × 1984; number of tomographies, 1440; number of slices, 1332; E = 40 kV, I = 200 μA; exposure time, 1.9 s. The slices reconstruction process and the correction of beam hardening and ring artifacts were achieved by means of commercial software (Cobra Exxim). Input projections and output slices are represented by files (one file per projection and one file per slice) using arrays of 16-bit integers. The segmentation of the slices was performed by the Otsu's method (Otsu, 1979), using Fiji software (Schindelin et al., 2012). BoneJ plugin (Doube et al., 2010) implemented on Fiji software was used for the analysis of the samples after the segmentation process.

2.4. Preparation of fluorescein labelled CTL (CTL-fluo) and confocal laser scanning microscopy of scaffolds

500 mg of CTL were dissolved in a final volume of 88.65 mL of deionized water and the pH was adjusted to 7 with NaOH. Subsequently 88 mL of sodium bicarbonate buffer (1 M) were slowly added to the solution. 100 μL of a 5 mg/mL FITC solution in sodium bicarbonate buffer (0.5 M) were added drop wise to the CTL solution to label 1/2000 of available amino groups. Then the mixture was dialyzed (dialysis membrane Spectrapore, MWCO 12000) three times against $NaHCO_3$ 0.05 M, two times against NaCl 0.1 M and against deionized water until the conductivity of the external solution was below 2 μS/cm at 4 °C. All procedures were carried out under dark condition. The solution was filtered through 0.45 μm filters and freeze dried. CTL-fluo was adsorbed on scaffold surface by soaking the scaffolds in a 0.2% w/V solution of CTL-fluo for 4 h. Scaffolds were then washed with deionized water and freeze-dried. Scaffolds containing CTL-fluo have been sectioned and analyzed with a Nikon Eclipse C1 microscope, coupled with an objective Nikon Plan Fluor 20× (2.10 WD, dry) using an argon laser (488 nm) and an acquisition channel of 515/30 nm. Images were analyzed with ImageJ software.

2.5. Attenuated Total Reflectance – Fourier Transform Infrared (ATR-FTIR) spectroscopy

ATR-FTIR was performed to analyze the presence of CTL and HAp within the scaffolds. IR spectra were acquired with a Nicolet 6700 spectrometer (Thermo Scientific, MI, Italy) within a wave number range of 4000–400 cm^{-1}. Three sample for each condition were analyzed, acquiring the spectrum with 32 scans and a resolution of 4 cm^{-1}.

2.6. Energy Dispersive Spectroscopy (EDS)

For the EDS analysis, samples were coated with a carbon layer using the Sputter Coater K550X coupled with the CA7625 Carbon Accessory (Emitech, Quorum Technologies Ltd., UK). Microanalysis was performed by Energy Dispersive Spectroscopy using an Apollo X EDAX probe (EDAX, Mawah, New Jersey, USA) coupled with the SEM (Quanta250 SEM, FEI, Oregon, USA); X-ray spectra were collected for 120 s.

2.7. Preparation of Simulated Body Fluid (SBF)

Evaluation of the in vitro scaffold stability was performed in SBF (Kokubo et al., 1990) with a pH of 7.4 and ion concentrations nearly equal to those of human blood plasma (Na^+ 142.0, K^+ 5.0, Mg^{2+} 1.5, $Ca2^+$ 2.5, Cl^- 147.8, HCO_3^- 4.2, HPO_4^{2-} 1.0, SO_4^{2-} 0.5 mM). SBF was prepared by dissolving reagent-grade chemicals of NaCl, $NaHCO_3$, KCl, K_2HPO_4, $MgCl_2{\cdot}6H_2O$, $CaCl_2$, Na_2SO_4 in distilled water and buffering at a pH of 7.4 with tris(hydroxymethyl)aminomethane $(CH_2OH)_3CNH_2$ and 1.0 M HCl at 36.5 °C.

2.8. Swelling and degradation behavior of scaffolds

The swelling behavior and the degradation of scaffolds were analyzed as previously reported (Porrelli et al., 2015; Turco et al., 2009), using Simulated Body Fluid (SBF).

The swelling behavior was quantified by measuring the changes in sample weight as a function of sample immersion time in SBF. Wet weights were determined after blotting with a filter paper to remove the surface liquid and the swelling ratio was calculated using the Eq. (1):

$$\text{Swelling}\ (\%) = \frac{\text{Ws–Wd}}{\text{Wd}} \times 100 \quad (1)$$

where W_d and W_s are the weights of the samples in the dry and the swollen state, respectively. The results were taken as the mean values of five samples for each condition.

Structural stability and integrity in SBF were evaluated during 5 weeks at 37 °C. The samples were immersed in 8 mL of SBF. Wet weight was measured after 10 min equilibration and at 1, 4, 7, 10, 14, 18, 21, 35 and 60 days of immersion. Soaking SBF was changed every 3 days. Weight variation was calculated using the Eq. (1):

$$\text{weight variation}\ (\%) = \frac{\text{1–Wtn}}{\text{W10}min} \times 100 \quad (2)$$

where W^{tn} and W^{10min} are the wet weights of the samples at the defined time and after 10 min of swelling, respectively.

2.9. CTL release evaluation

Alginate scaffolds were coated with CTL-FITC as described above (Section 2.1). After the adsorption process, the fluorescence of the CTL-FITC solution was measured, in order to determine the amount of adsorbed CTL-FITC. Then, the amount of CTL-FITC released from the scaffolds in SBF was determined at different time points (1, 3, 6 24, 48, and 72 h), incubating CTL coated scaffolds with 1.5 mL of SBF, changing the solution at each time point and measuring its fluorescence intensity. Fluorescence intensity measures were performed with the GloMax Multi+ Detection System spectrofluorometer (Promega, Madison, WI, USA) using an excitation wavelength of 490 nm and collecting the fluorescence emission in the range 510–570 nm.

2.10. Uniaxial compression tests of hydrogels and scaffolds

Mechanical tests were performed on scaffolds soaked in SBF following the same approach used for the degradation tests. Compression tests have been performed with a Universal Testing Machine (Galdabini Sun 500, Cardano al Campo, VA, Italy) equipped with a 100 N load cell. A constant compression speed of 1 mm/min was used up to 60% of sample strain. For each type of scaffold, 5 replicates were averaged. The compression modulus, the compression strength and the toughness at 60% of strain were determined. The compressive modulus was calculated from the initial linear range of the stress strain curves (from 2 to 5% of strain).

2.11. Human dental pulp stem cells isolation

Freshly extracted, non-carious, human third molars were collected from surgical patients (Authorization by Regional Health Service - Azienda Sanitaria Universitaria Integrata di Trieste and by the Comitato Etico Unico Regionale - CEUR FVG, ID studio 2433: TERM – “Collection

of biological samples for the study of biocompatibility and bioactivity on dental pulp cells of materials for restorative and regenerative dentistry"). The teeth were placed into PBS containing antibiotics (500 U/mL penicillin, 500 mg/mL streptomycin) and were immediately transferred to laboratory for pulp isolation. Two types of enzyme solutions were prepared: 12 mg/mL of Collagenase I (50–200 U/mL, Life technology) in PBS and a 16 mg/mL of Dispase II (50 U/mL, Merck) in PBS. Both mixtures were sterilized by filtering the solutions using a 0.2 μm syringe filter. The pulp chamber of the teeth was exposed under sterile conditions in a biohazard laminar flow hood, using a microtome (IsoMetTM Low Speed Saw, BUEHLER, China). The entire pulp tissue was cut into small pieces with a scalpel blade and transferred in to a Petri dish with 2 mL of the proteolytic enzymes for 45 min at 37 °C. Afterwards, the digested cell suspension was transferred in a 15 mL falcon tube with 3 mL of Dulbecco's Modified Eagle Medium (DMEM) supplemented with 2% glutamine, 500 U/mL penicillin, 500 mg/mL streptomycin and 10% fetal bovine serum (FBS) and centrifuged at 180 ×*g* for 5 min at room temperature. The cell pellet was then resuspended in complete DMEM containing L-ascorbic acid 2-phosphate 100 μM and seeded into 25 cm^2 culture flask at 37 °C and 5% pCO_2 (partial pressure of CO_2 in the incubator). The culture medium was changed every three days until 80% of cell confluence was achieved. Cells were always subcultured at confluence of 70–80% using trypsin digestion.

2.12. CTL effects on cell proliferation

Cells were cultured in complete DMEM with ascorbic acid 100 μM, in a 24-well plate in a humidified atmosphere of 5% pCO_2 at 37 °C. After 1 day of incubation, culture medium was substituted with complete DMEM with ascorbic acid 100 μM and CTL at three different concentrations (0.05%, 0.1% and 0.2% w/V, starting from a sterile stock solution of CTL in PBS 1.5% w/V); as control, the same volume of PBS was added to DMEM. After 1, 3, 6 and 8 days, cell proliferation was tested by Alamar Blue assay: cells were washed with PBS and incubated with 100 μL of 10% Alamar Blue in DMEM, for 4 h in darkness, at 37 °C. The medium was then collected from each well and replaced with fresh medium; the fluorescence of the collected medium was measured (λ_{exc} = 544 nm; λ_{em} = 590 nm) with a spectrofluorimeter (FLUOstar Omega, BMG LABTECH, Germany).

2.13. Alizarin red S staining

Alizarin red S staining solution was prepared dissolving 2 g of Alizarin Red S powder (M.W. 342.26 Da, Merck) in 100 mL of distilled water and buffering at pH 4.1–4.3 with 10% w/V ammonium hydroxide. After 21 days cells were washed with PBS and fixed by 1 mL/well of 10% v/V paraformaldehyde in PBS for 15 min at RT. Then paraformaldehyde was removed carefully, and cells were washed 3 times (5–10 min for each time) with deionized water without disturbing the monolayer. After washing, 1 mL/well of Alizarin Red S solution was added for 20 min at RT. Cells were then washed with deionized water four times (5 min for each time with gentle shaking) to remove any additional Alizarin Red. 1 mL/well of distilled water was added to prevent the cells from drying and an image acquisition was taken with an optical microscope.

2.14. Determination of alkaline phosphatase activity on 2D cell culture

A suspension of 1000 cells was seeded into each well of a 6-well plate with complete DMEM plus ascorbic acid 100 μM and maintained in culture at 37 °C in a 5% pCO_2 atmosphere. After 1 day of culture, the medium was replaced with complete DMEM with ascorbic acid 100 μM and with CTL 0.2% w/V (starting from a sterile stock solution of CTL in PBS 1.5% w/V), with a differentiation mixture (dexamethasone 10 nM, β-glycerol phosphate disodium salt pentahydrate 5 mM and potassium phosphate monohydrate 1.8 mM; here indicated as "DS", for "differentiation stimuli"), or with differentiation mixture and CTL. The media were replaced every 3 days. At 1 and 17 days, cells were washed at room temperature for 30 min in a buffer 10 mM HEPES, pH 7.4, containing 10 mM $CaCl_2$, 100 mM NaCl, 5 mM glucose. Cells were lysed in a lysis buffer (TritonX-100 0.2% w/w in Tris/HCl 100 mM, pH 9.8) and stored for 30 min at −80 °C. Enzymatic activity was evaluated in the lysate with a reaction buffer (para-nitro-phenyl-phosphate 6 mM, $MgCl_2$ 1 mM, in Tris-HCl 100 mM, pH 9.8) after 60 min of incubation at 37 °C. Absorbance was measured at 410 nm with a Tecan Nano Quant Infinite M200 Pro plate reader. The results were normalized to the number of cells determined by Alamar Blue assay.

2.15. Cell adhesion on scaffolds

Scaffolds (with or without adsorbed CTL) were sterilized with UV light (20 min per cycle, 3 cycles) (Marsich, Bellomo, et al., 2013; Marsich, Travan, et al., 2013; Porrelli et al., 2015). Scaffolds were then conditioned in a sterile water solution containing $CaCl_2$ 5 mM (in order to further stabilize the structure for the biological experiments), 100 U/mL penicillin and 100 μg/mL streptomycin for 20 min and then placed in 24-well plates with complete DMEM with ascorbic acid 100 μM and incubated for 24 h at 37 °C and 5% pCO_2. A suspension of 40,000 cells in 40 μL has been placed on each scaffold and left 4 h to ensure cell adhesion; after 4 h complete DMEM with ascorbic acid 100 μM was added to each scaffold and the cells have been incubated for 24 h at 37 °C and 5% pCO_2. After 24 h, cell adhesion was assessed by means of the Alamar Blue assay as previously described.

2.16. Cell proliferation on scaffolds

Scaffolds were sterilized and conditioned as above described. A suspension of 40,000 cells in 40 μL has been placed on each scaffold and left 4 h to ensure cell adhesion; after 4 h complete DMEM with ascorbic acid 100 μM was added to each scaffold and the cells have been incubated at 37 °C and 5% pCO_2. Medium was replaced every 2 days. MTS assay was performed at 1, 7 and 14 days. Briefly, after 4 h of incubation with the MTS reagent (10% w/V in complete DMEM), the medium was collected and absorbance was measured with a *Nano Quant Infinite M200 Pro* (Tecan, Swiss) plate reader at a wavelength of 490 nm. The background absorbance obtained from an empty scaffold (blank) was subtracted from the sample values.

2.17. Determination of alkaline phosphate activity on 3D cell culture

Scaffolds were sterilized and conditioned as above described. A suspension of 40,000 cells in 40 μL has been placed on each scaffold and left 4 h to ensure cell adhesion; after 4 h complete DMEM with ascorbic acid 100 μM was added to each scaffold and the cells have been incubated at 37 °C and 5% pCO_2. After 24 h, the medium was replaced on both Ctrl-sc and CTL-sc, which were divided in two subgroups: a group cultured with DMEM added with ascorbic acid 100 μM and a group cultured with DMEM added with ascorbic acid 100 μM and DS; medium was then changed every 2 days. ALP activity was evaluated at 1 and 17 days: scaffolds were washed at room temperature for 30 min in a washing buffer (HEPES 10 mM, $CaCl_2$ 10 mM, NaCl 100 mM, glucose 5 mM, pH 7.4). Cells were lysed adding a lysis buffer to the scaffolds (TritonX-100 0.2% w/w in Tris/HCl 100 mM, pH 9.8) and keeping the scaffolds for 30 min at −80 °C. Enzymatic activity was measured in a reaction buffer (para-nitro-phenyl-phosphate 6 mM, $MgCl_2$ 1 mM, in Tris-HCl 100 mM, pH 9.8) after 60 min of incubation at 37 °C. Absorbance was measured at 410 nm with a Tecan Nano Quant Infinite M200 Pro plate reader. The results were normalized to the number of cells determined with the MTS proliferation assay, performed as described above.

2.18. Scanning electron microscopy (SEM) of scaffolds

Scaffolds seeded with cells were washed with 10 mM HEPES, pH 7.4, containing 10 mM $CaCl_2$, 100 mM NaCl, and 5 mM glucose and fixed with 10% glutaraldehyde in PBS for 1 h at room temperature. Samples were then washed three times with the same buffer described above. Samples were then dehydrated by stepwise treatment with ethanol in water (30%, 50%, 70%, 90%, 100%), and then with hexamethyldisilazane in ethanol (30%, 50%, 70%, 90%, 100%). After 1 h in hexamethyldisilazane 100% samples were air-dried, sputter-coated with gold (Sputter Coater K550X, Emitech, Quorum Technologies Ltd., UK), and visualized by scanning electron microscopy (Quanta250 SEM, FEI, Oregon, USA) operated in secondary electron detection mode. The working distance was adjusted in order to obtain the suitable magnification; the accelerating voltage was set to 30 kV.

2.19. Statistical analyses

Statistical analyses were performed by means of Origin software (OriginLab Corporation). Data that satisfied both the normality (Kolmogorov–Smirnov test) and equality variance (Levene test) assumptions were analyzed with one-way ANOVA test, applying Bonferroni correction. Data that did not satisfy normality and equality of variance were analyzed by Kruskal-Wallis and by Mann–Whitney non-parametric tests. Statistical significance was pre-set at $\alpha = 0.05$.

3. Results

3.1. CTL effects on cells

The biological effect of CTL presence on hDPSCs cultures was studied in terms of cell proliferation. Characterization of stemness of hDPSCs and of the expression of Galectin 1 is reported in Supplementary Materials. CTL was diluted in culture medium, and the hDPSCs proliferation rate was monitored using the Alamar Blue assay. The results, reported in Fig. 1A, demonstrate the high replication rate of hDPSCs reaching a proliferation plateau after 3 and 5 days. CTL has not significant effect on cell proliferation, even if a slight positive effect was observed.

The effects of CTL on the differentiation of hDPSCs were investigated analyzing the alkaline phosphatase (ALP) activity and the deposition of mineralized matrix. Cells were cultured in the presence of CTL and/or Differentiation Stimuli (DS) and tested at different time points. ALP activity was analyzed measuring the amount of para-nitro-phenyl-phosphate converted by the enzyme after 1 and 17 days of culture (Fig. 1B). At day 1, ALP activity was not detectable for all the tested conditions, whereas after 17 days of culture, depending on the treatment, an increase of ALP activity was observed. A slight increase of ALP activity could be observed also for Ctrl cells, probably due to an initial cell commitment caused by cell confluence. As expected, a statistically significant increase was evident in cells cultured in the presence of DS (differentiation stimuli) and CTL-DS compared to Ctrl cells. A smaller increase, which was not significantly different compared to Ctrl cells, was also observed for cells cultured in the presence of CTL. Noteworthy, the ALP activity in cells cultured in presence of both CTL and DS is significantly higher of ALP activity observed in cells treated with only DS.

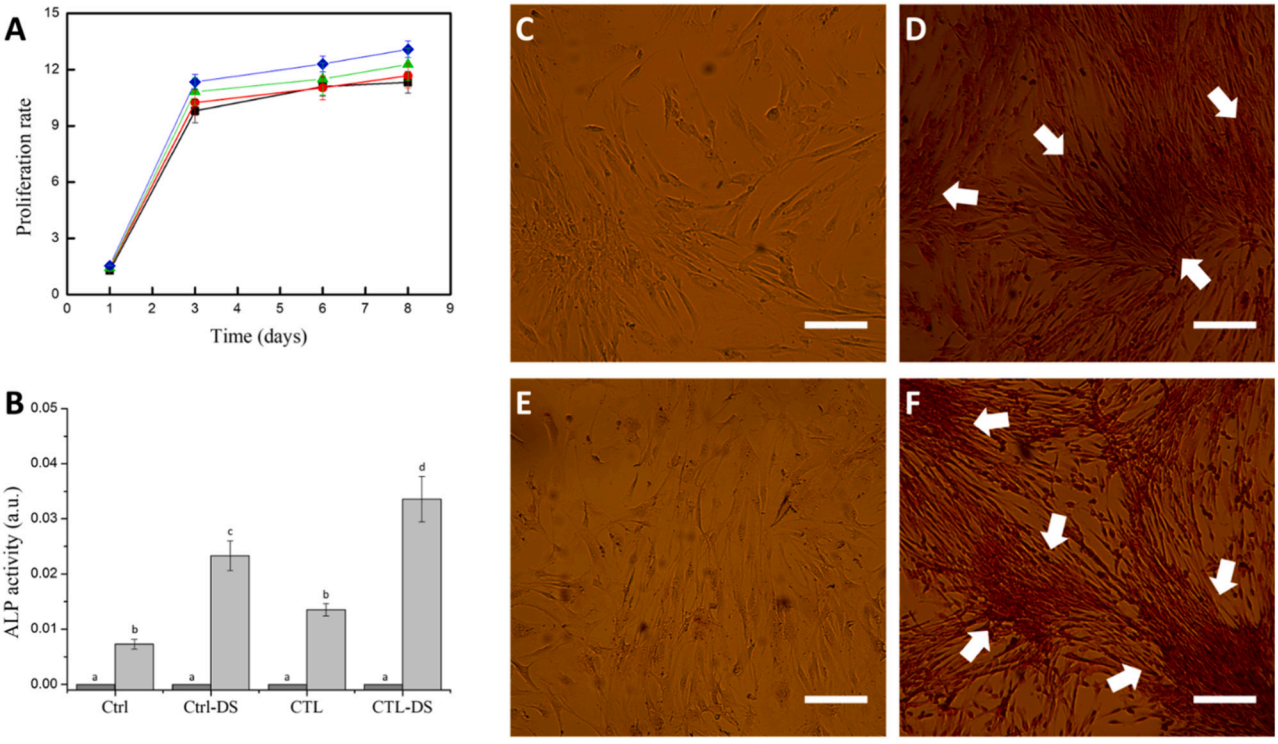

Fig. 1. Biological properties of CTL. A) CTL effects on hDPSCs proliferation. Proliferation rate for hDPSCs cultured without CTL (■) or with CTL at different concentrations: 0.05% w/V (●), 0.1% w/V (▲) or 0.2% w/V (◆). Error bars represent standard deviations. B) CTL effects on differentiation of hDPSCs. ALP activity at 1 (dark grey bars) and 17 (light grey bars) days of hDPSCs cultured without (Ctrl) and with CTL (CTL), differentiation stimuli (Ctrl-DS) and with CTL and differentiation stimuli (CTL-DS). Statistical analyses were performed by one-way ANOVA test using Tukey's correction. The absence of statistically significant differences is indicated with the same lowercase letter, vice versa, different letters are used. Ctrl vs Ctrl-DS, $p < 0.001$; Ctrl vs CTL, $p > 0.05$; Ctrl vs CTL-DS, $p < 0.001$; Ctrl-DS vs CTL, $p = 0.007$; Ctrl-DS vs CTL-DS, $p = 0.005$; CTL vs CTL-DS, $p < 0.001$. Error bars represent standard deviations. CTL effects on extracellular matrix deposition. Optical microscope observation of Alizarin Red stained cells, cultured in control medium (C) or in the presence of DS (D), CTL (E), and CTL + DS (F). White arrows in Fig. 5B and D indicate the red staining of mineralized extracellular matrix. Scale bar is 100 μm.

Deposition of mineralized extracellular matrix was assessed by Alizarin Red assay after 14 and 21 days of culture in presence of CTL, DS, or both. After 14 days of culture (figures not shown), no mineral deposition was detectable; after 21 days, calcium deposition, indicated by white arrows, could be easily observed for hDPSCs cultured in the presence of DS (Fig. 1D) and in the presence of CTL and DS (Fig. 1F).

3.2. Scaffolds preparation and characterization

Fig. 2 reports a schematic of the scaffolds manufacturing process. Three-dimensional porous scaffolds were obtained by freeze-drying alginate/hydroxyapatite hydrogels, prepared using a slow gelation method (Turco et al., 2009). After freeze-drying, scaffolds (Ctrl-sc) were soaked in a CTL solution to adsorb the bioactive polymer onto the scaffold trabeculae. The scaffolds underwent to a second freeze-drying process (thus obtaining CTL-sc). The porous structure of the scaffolds and the similarity between Ctrl-sc and CTL-sc can be seen from the SEM micrographs reported in Fig. 3A and B.

Micro-computed tomography (μ-CT) was performed on both Ctrl-sc and CTL-sc in order to characterize their structures and to analyze the effects of CTL adsorption and of the second freeze-drying process. Moreover, confocal laser scanning microscopy (CLSM), was performed on CTL-sc prepared with fluoresceine-labelled CTL, to confirm the uniform adsorption of CTL within the scaffold structure. Fig. 3 and Table 1 show the results of the morphological analyses performed on the scaffolds. μ-CT analysis revealed that the adsorption of CTL and the second freeze-drying process do not change the three-dimensional structure of CTL-sc (Fig. 3C) compared to Ctrl-sc (Fig. 3D). These findings are confirmed by the quantitative analysis (Table 1), that revealed only a slight increase of scaffolds porosity and trabecular spacing (pore diameter).

The three-dimensional reconstruction obtained from CLSM analysis of an inner part of CTL-sc, is reported in Fig. 3E. The analysis shows that CTL is able to infiltrate into the structure and adsorb uniformly onto the trabeculae. CLSM imaging of Ctrl-sc is not reported since it was not possible to detect a background fluorescence signal.

Attenuated Total Reflectance – Fourier Transform Infrared (ATR-FTIR) spectroscopy and Energy Dispersive Spectroscopy (EDS) have been performed on Ctrl-sc and CTL-sc in order to analyze their chemical structure. The EDS spectra of HAp, Ctrl-sc and CTL-sc are reported in Fig. 4A, B and C respectively and confirm the presence of calcium and phosphorus within the scaffolds; Ca/P ratio is reported in Fig. 4D and is similar between the analyzed scaffolds and the hydroxyapatite.

Infrared spectra of Ctrl-sc and CTL-sc are reported in Fig. 4E and compared to the spectra obtained for alginate, CTL and HAp. Analyzing the spectra obtained for the scaffolds it is possible to appreciate the specific signals of HAp and also the signals of the polysaccharides; in particular, for CTL-sc, the infrared band of the hydroxyl groups is more intense with respect to Ctrl-sc, confirming the presence of CTL coating.

The stability of CTL coating was investigated analyzing its release from CTL-sc soaked in Simulated Body Fluid (SBF). The cumulative release profile is reported in Fig. 5A and shows that after a burst release of CTL of about 30% (over the total contained in the scaffold), a plateau of 65% of release is reached after 10 h. The swelling behavior of the scaffolds soaked in SBF is reported in Fig. 5B; the graph shows that there are not differences between the behavior of Ctrl-sc and CTL-sc and that the structures rapidly swell in the first minutes of the experiment; reaching the maximum of swelling (~1850%) after 1 day. The stability of Ctrl-sc and CTL-sc was analyzed in terms of weight and mechanical property variations over a period of 60 days, soaking the scaffolds in SBF in order to test the scaffolds in physiological-like conditions. The weight variation of the scaffolds is reported in Fig. 5C: Ctrl-sc and CTL-sc show a similar behavior up to 20 days, but after this time point, the degradation rate of Ctrl-sc is faster than CTL-sc one. At 60 days, the difference between Ctrl-sc and CTL-sc weight is statistically significant. This difference could be due to two distinct contributions: the presence of CTL,

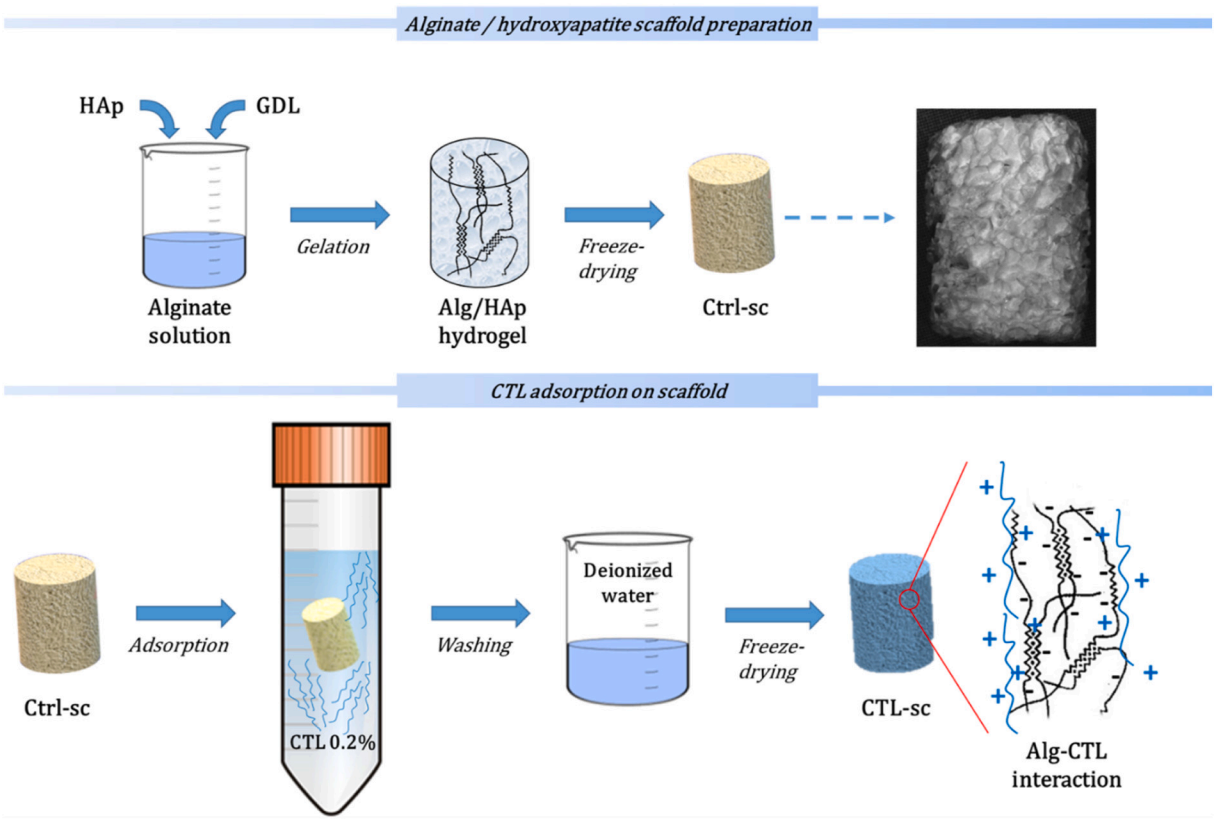

Fig. 2. Schematic representation of the scaffolds manufacturing process, and of the scaffolds coating with CTL.

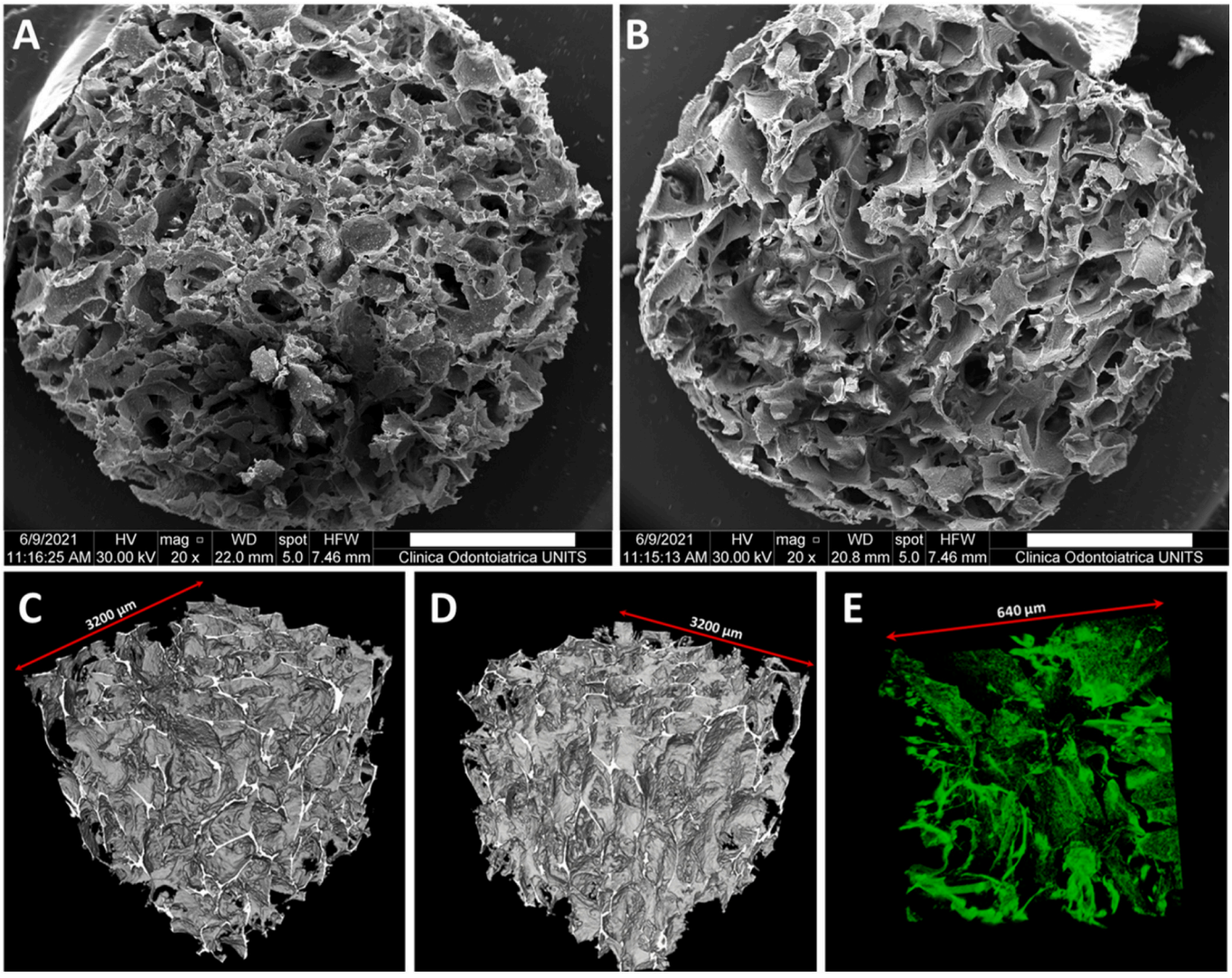

Fig. 3. Morphological characterization of scaffolds. SEM analysis of Ctrl-sc (A) and CTL-sc (B); scale bar is 2 mm. Three-dimensional reconstructions of Alg/HAp scaffolds without (C) or whit (D) CTL, determined with micro-computed tomography. In figure E the three-dimensional reconstruction, determined with confocal laser scanning microscopy, of scaffold containing fluoresceine-labelled CTL is reported.

Table 1
Quantitative characterization of the microstructure of the alginate scaffolds.

	Ctrl-sc	CTL-sc
Porosity	88.3% ± 0.5%	89.8 ± 0.7%
Mean Tb.Th (µm)	43 ± 14	42 ± 14
Mean Tb.Sp (µm)	349 ± 138	366 ± 142
Conn.D (μm^{-3})	1.1E−07 ± 0.2E−07	0.8E−07 ± 0.2E−07
DA	0.66 ± 0.01	0.51 ± 0.04

Tb.Th.: Trabecular Thickness; Tb.Sp.: Trabecular Spacing; Conn.D: Connectivity Density; DA: Degree of Anisotropy. Data are given ± s.d. (four experiments). Linear resolution is 8 µm.

which act as a cross-linker between alginate chains, and to the second freeze-drying process, which stabilize the structure. The mechanical properties of SBF soaked scaffolds were analyzed through uniaxial compression tests, which were performed up to the 60% of deformation, since it was not possible to reach the failure of the hydrated structures. The compression modulus, calculated with a linear fitting from 2 to 5% of deformation, is reported in Fig. 5D; the stress and the toughness reached by the structures, at 60% of deformation, are reported in Fig. 5E and F. A decrease in the mechanical performances of the scaffolds, of about the 50%, can be observed up to 10 days. After this time point, the decrease is negligible and the structures maintain their stability.

3.3. *Influence of CTL coating on cells*

The influence of CTL adsorbed within the scaffolds was tested in terms of cell adhesion, proliferation, and differentiation. Ctrl-sc and CTL-sc were UV sterilized and conditioned with culture medium prior to cells seeding. Cell adhesion was evaluated 24 h after seeding by Alamar Blue assay; results reported in Fig. 6A show that the intensity of fluorescence signal of CTL-sc is significantly higher than that of Ctrl-sc, indicating a higher number of adhered cells.

Cell proliferation of hDPSCs seeded within scaffolds was tested with an MTS assay up to 14 days (Fig. 6B). The proliferation rate of hDPSCs seeded in Ctrl-sc and in CTL-sc was comparable ($p > 0.05$ for all days), although the presence of CTL increased the adhesion of cells within the scaffolds. Moreover, the 3D structure increases the cell adhesion surface with respect to 2D culture dish, resulting in a linear proliferation trend, which does not reach a plateau after 14 days of cell culture.

After 2 days of cell culture, Ctrl-sc and CTL-sc were fixed, dehydrated, and observed with SEM in order to evaluate the ability of cells to colonize the scaffolds. Fig. 6 reports two micrographs of the exposed

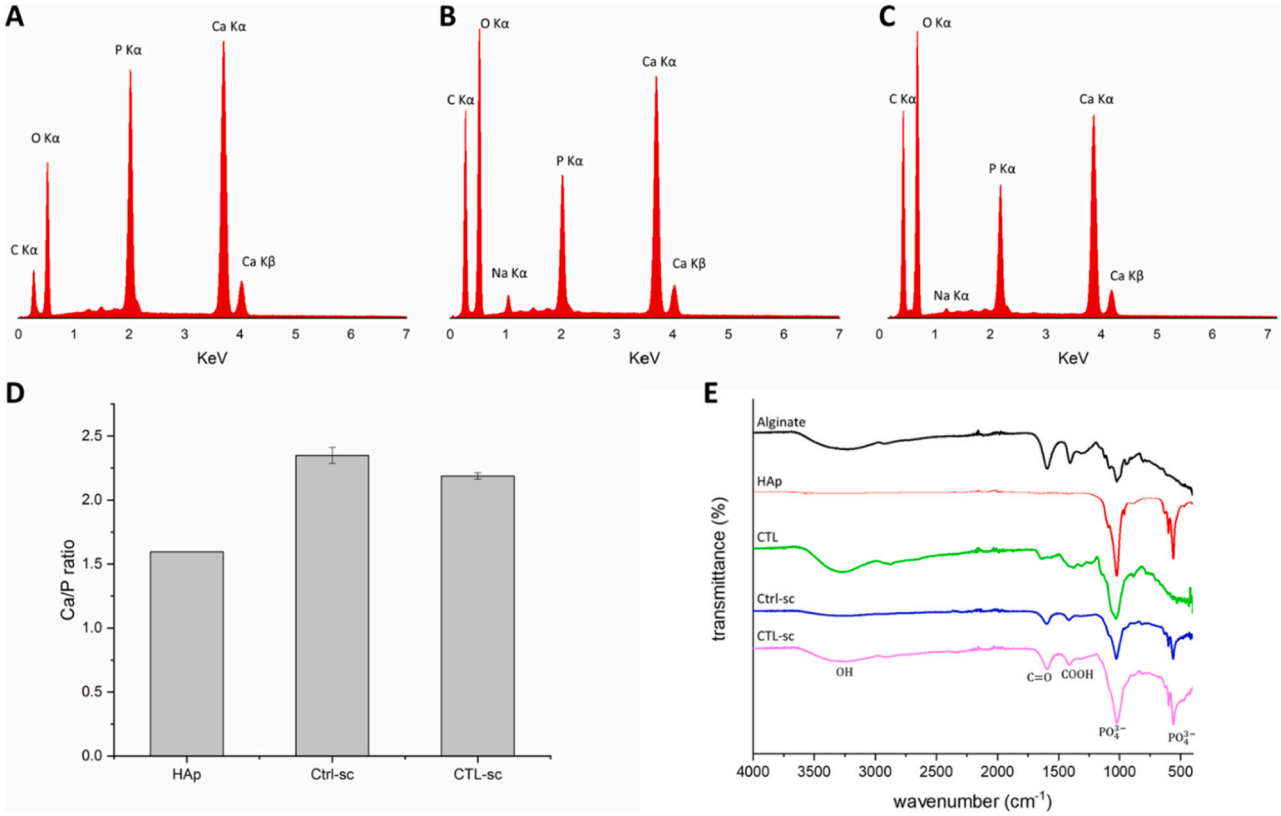

Fig. 4. Chemical characterization of the scaffolds. EDS spectra of hydroxyapatite (A), Ctrl-sc (B) and CTL-sc (C). In figure D the Ca/P ratio is reported, there are not significant statistical difference between the ratios. In figure E the infrared spectra of Ctrl-sc and CTL-sc are compared with those of pure alginate, pure CTL and pure HAp.

internal structure of the scaffolds. It is possible to appreciate clusters of cells grown on scaffold trabeculae for both Ctrl-sc (6C) and CTL-sc (6D). In particular, hDPSCs appeared well integrated within the 3D structure and it is possible to appreciate an initial matrix deposition.

The ability of CTL to affect cell differentiation towards osteoblast phenotype was assessed in scaffolds with or without CTL, and in presence or not of DS. To this end, ALP activity was tested on cells grown on Ctrl-sc and CTL-sc in presence and absence of DS. The results reported in Fig. 6E show that, as already observed for 2D cell culture, CTL does not induce ALP expression, which is not significantly different with respect to Ctrl scaffolds. On the contrary, it is interesting to note that the combination of CTL and DS results in a strong synergistic effect on ALP activity that is almost fourfold the one observed for scaffold in presence of DS but without CTL.

4. Discussion

Three-dimensional porous scaffolds are a promising tool for bone tissue engineering applications (Asghari Sana et al., 2017; Sancilio et al., 2018; Sharma et al., 2016). The use of polysaccharides allows to prepare biocompatible and bioactive scaffolds, which can be tailored in order to properly tune their morphological and biological properties (Sharma et al., 2016). In this work, three-dimensional porous scaffolds were prepared with alginate and hydroxyapatite, and functionalized with a bioactive chitosan derivative (CTL). As previously reported, the protocol applied enable to obtain highly porous and highly interconnected matrices (Marsich, Bellomo, et al., 2013; Porrelli et al., 2015; Turco et al., 2009). The structures were functionalized by physical adsorption of CTL on the scaffold trabeculae. Such adsorption is mainly due to the ionic interactions between the positive charges carried by CTL (on nitrogen atoms) and the negative charges carried by alginate as depicted in Fig. 2 (on carboxylic groups) (Marsich, Bellomo, et al., 2013; Marsich, Travan, et al., 2013). Both ATR-FTIR and EDS analyses confirmed the presence of HAp and CTL within the scaffolds. The stoichiometric Ca/P ratio, which can be used to evaluate the presence of HAp (Turco et al., 2018), is slightly higher for Ctrl-sc and CTL-sc with respect to pure HAp: this result could be due to the HAp dissociation and Calcium retainment in the alginate egg-box structures, caused by the ionic gelation. CLSM imaging confirmed that the adsorption process guarantees a homogeneous coating of scaffold trabeculae with CTL. μ-CT analysis demonstrated that the CTL adsorption and the second freeze-drying process, mandatory to obtain dry structures, do not alter the morphological and structural features of the scaffolds, which were claimed to be suitable for bone tissue regeneration (Panzavolta et al., 2013; Sharma et al., 2016).

The stability and the mechanical properties of biodegradable scaffolds are essential to match the biological processes of cell adhesion and colonization of the scaffolds, and of cell differentiation and extracellular matrix deposition (Asghari Sana et al., 2017; Sancilio et al., 2018; Sharma et al., 2016). The stability of CTL coating was confirmed by the evaluation of the release profile; in particular, even if a burst release of CTL was observed during the first hours (which could act in solution on cells), a high amount of CTL remains adsorbed on the scaffold trabeculae, ensuring its bioactivity in the long term. The hydrophilicity of the structures and their ability to uptake fluids are important for the proper interaction between the scaffold and the surrounding tissue to ensure cell migration and scaffold colonization (Podporska-Carroll et al., 2014). The swelling tests showed that the scaffolds are highly hydrophilic and able to uptake a large amount of fluid in a similar way to what has been already observed for alginate/hydroxyapatite scaffolds (Porrelli et al., 2015; Turco et al., 2009).

The stability of scaffolds was tested after incubation at 37 °C in Simulated Body Fluid, mimicking physiological conditions (Kokubo

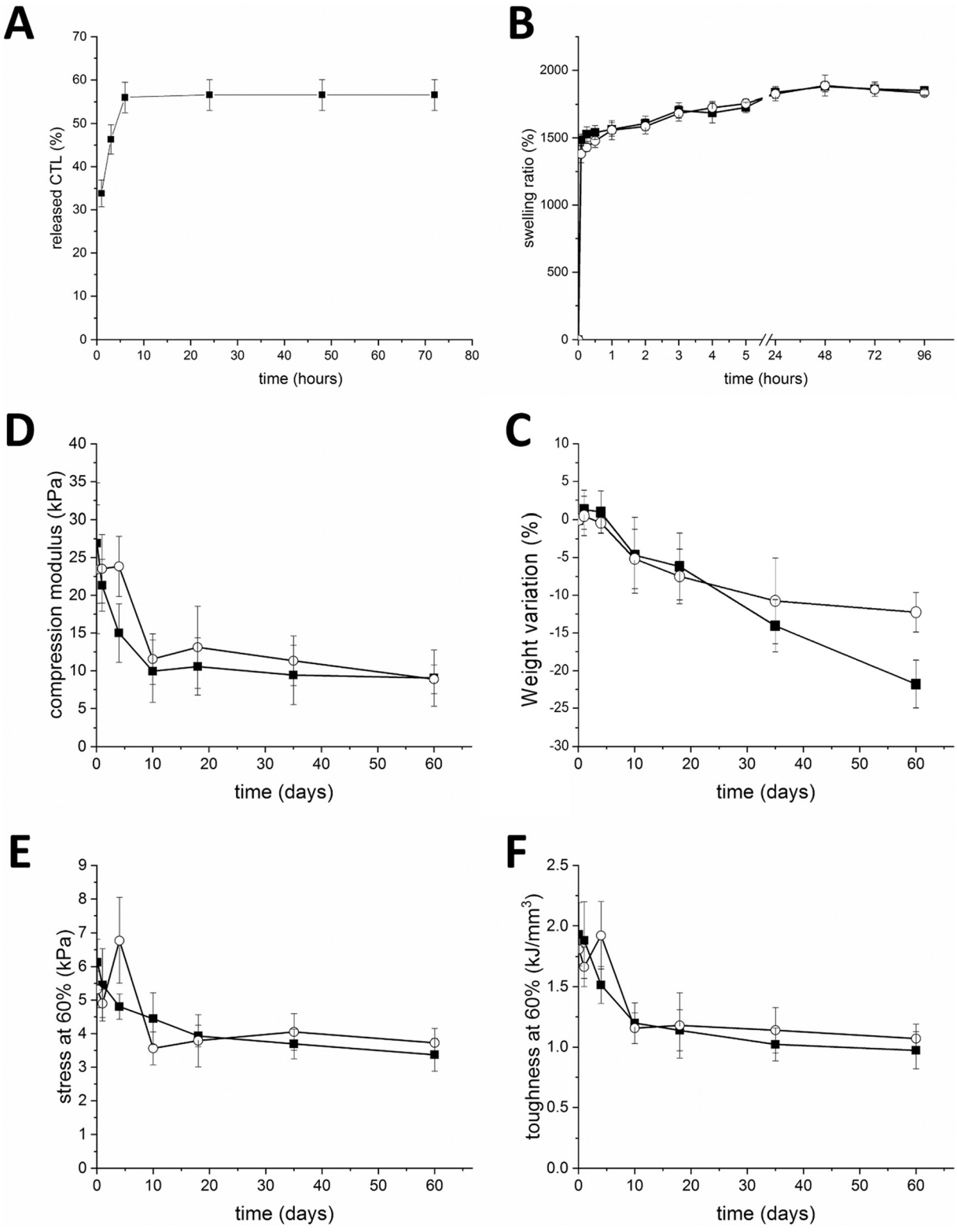

Fig. 5. Scaffolds stability and mechanical properties. (A) Profile of CTL cumulative release in SBF. (B) Swelling profile of Ctrl-sc (■) and CTL-sc (○) in SBF. (C) Stability of Ctrl-sc (■) and CTL-sc (○)after incubation in Simulated Body Fluid at 37 °C expressed as percentage of scaffold mass lost during incubation. The difference between scaffold weights at 60 days is statistically significant ($p < 0.05$). In (D) elastic compression modulus in (E) stress at 60% of strain, and in (F) toughness at 60% of strain of Ctrl-sc (□) and CTL-sc (○).

et al., 1990). The weight variation observed over time was more pronounced for Ctrl-sc with respect to CTL-sc. Weight loss is mostly caused by monovalent cations of SBF, which tend to substitute Ca^{2+}, and dissolve the alginate "egg-box" structures that stabilize the polymer network. The addition of CTL, which can act as a cross-linker between alginate chains thanks to its polycationic nature as depicted in Fig. 2 (Medelin et al., 2018), should slow the dissolution of the egg-boxes and thus stabilize the alginate scaffolds, similar to what is observed for

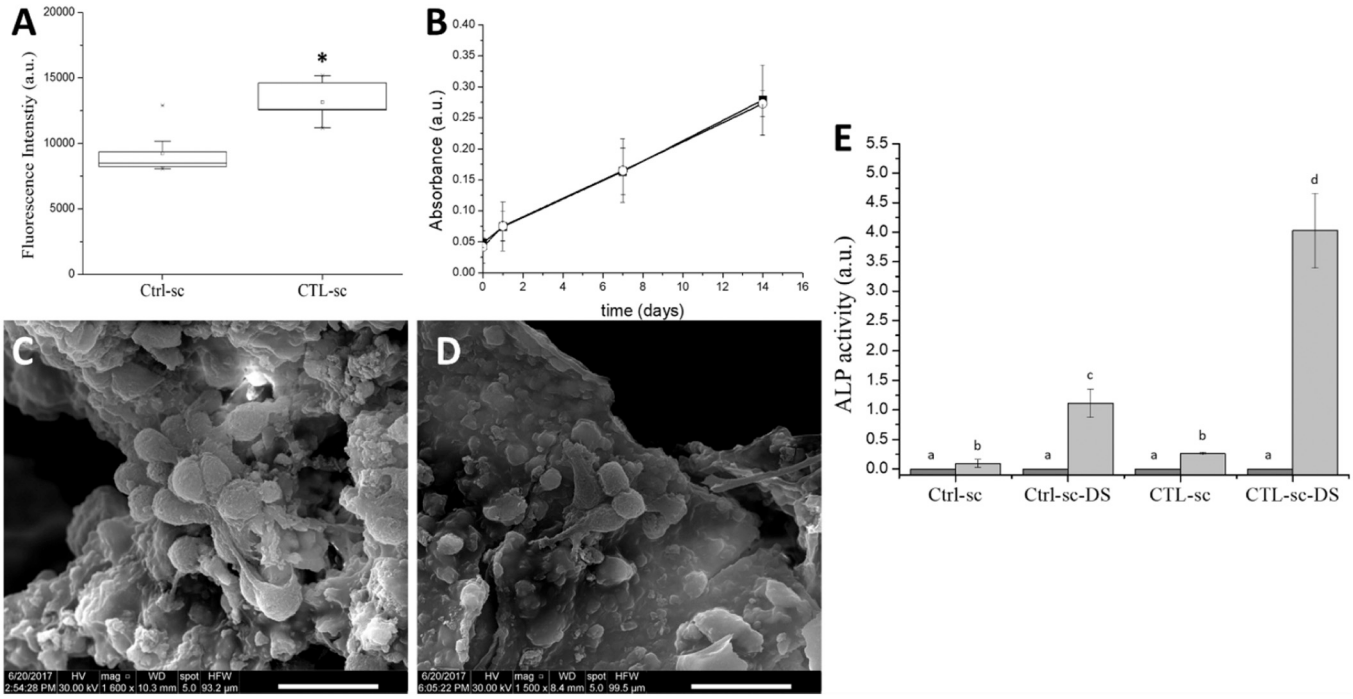

Fig. 6. CTL coating effects on hDPSCs adhesion and proliferation. A) Fluorescence intensity of Alamar Blue assay, measured in order to evaluate hDPSCs adhesion within Ctrl-sc and CTL-sc after 24 h. Statistically significant difference was determined with Mann-Withney *U* test ($p < 0.05$). B) Proliferation of hDPSCs seeded in Ctrl-sc (■) and CTL-sc (○), measured tested MTS assay. In (C) and (D) SEM micrographs of hDPSCs seeded in Ctrl-sc (C) and CTL-sc (D). Scale bar, 20 μm. E) Influence of CTL coating on hDPSCs differentiation. ALP activity of hDPSCs in Ctrl-sc and CTL-sc, with or without differentiation stimuli (DS) at 1 (dark grey bars) and 17 (light grey bars) days. Statistical analyses were performed by means of one-way ANOVA test applying Tukey's correction. The absence of statistically significant differences is indicated with the same lowercase letter, vice versa, different letters are used. Ctrl-sc vs Ctrl-sc-DS, $p < 0.001$; Ctrl-sc vs CTL-sc, $p > 0.05$; Ctrl-sc vs CTL-sc-DS, $p < 0.001$; Ctrl-sc-DS vs CTL-sc, $p < 0.05$; Ctrl-sc-DS vs CTL-sc-DS, $p < 0.001$; CTL-sc vs CTL-sc-DS, $p < 0.001$. Error bars represent standard deviations.

alginate-chitosan scaffolds (Li et al., 2005). Despite the increased stability of CTL-sc with respect to Ctrl-sc, mechanical properties of the two types of scaffolds are similar: mechanical resistance (calculated as stress and toughness sustained at 60% of deformation) and compression modulus of both scaffolds decrease by half in about 10 days; successively a slow and negligible decrease of mechanical properties can be observed until the 60th day of the experiment. The variation of the mechanical properties of the scaffolds reaches a plateau after 10 days: this could be due to the fact that after this time point the contribute of water entrapped in scaffold pores become predominant over the contribute of the scaffold itself; this consideration can explain the differences observed between the trends of the mechanical properties and the degradation rate. The mechanical behavior, and in particular the variation of the elastic modulus over time, allows to exclude a detectable precipitation of ions from SBF, as already reported in a previous work (Porrelli et al., 2015). The stability of the structures is able to guarantee cell adhesion and colonization of the scaffolds; moreover, it is compatible with the required time for cell proliferation and differentiation, and with the deposition of extracellular matrix (Ghanaati et al., 2011; Hutmacher, 2000; Park et al., 2010; Urist, 1965). The mechanical properties of the scaffolds described here are not comparable to those of the native bone tissue (Misch et al., 1999); therefore the scaffolds must be intended to be used as void fillers, e.g., in Guided Bone Regeneration (Battafarano et al., 2021; Zhao et al., 2021). The biological properties of CTL-functionalized alginate scaffolds were assessed using hDPSCs; these mesenchymal stem cells derived from the human dental pulp, under proper stimuli, can differentiate in osteoblasts, chondroblasts, fibroblasts, adipocytes and neurons (Aimetti et al., 2018; Kanafi et al., 2014; Karadzic et al., 2015; Mata et al., 2017; Tatullo et al., 2015). Moreover, their employment allows to prepare personalized cell-loaded scaffolds, which could be used for autologous cell therapies; in this context, dental pulp stem cells have been used for the regeneration of pulp tissue (Bhoj et al., 2015), periodontal tissue in infrabony defects (Aimetti et al., 2014; Aimetti et al., 2018), bone tissue in mandibular distraction osteogenesis (Alkaisi et al., 2013) and cartilage tissue (Mata et al., 2017). In this work, hDPSCs were obtained by enzymatic digestion of dental pulp collagen; FACS analyses showed that the isolated cell population was highly enriched with mesenchymal stem cells, without hematopoietic cells. ELISA tests confirmed the expression of Galectin-1 in hDPSCs (Akpinar et al., 2014). The presence of Galectin-1 is of paramount importance for the use of glycosylated bioactive polymers like CTL (Camby et al., 2006; Liu et al., 2018; Marcon et al., 2005): it was showed that Galectin-1 mediates the interactions between cells and glycosylated macromolecules, triggering several biological processes like cell adhesion, proliferation, differentiation and extracellular matrix deposition (Kadri et al., 2005; Tazhitdinova & Timoshenko, 2020). Moreover, Galectin-1 has been found to be involved in the differentiation of human BMSCs towards and osteoblast phenotype (Andersen et al., 2003) and is associated with the maturation of osteoblasts (Choi et al., 1998). The involvement of Galectin-1 in the biological processes mediated by CTL is already known from tests performed on chondrocytes; moreover, it was recently showed that Galectin-1 is able to bind CTL (Liu et al., 2018). As already assessed (Furlani et al., 2019), hDPSCs proliferation is not affected by the presence of CTL, here tested both in solution and as scaffold coating. Regarding the biological effects of CTL in solution, this polymer is not able to promote cell proliferation, but, in presence of differentiation agents, it is able to stimulate the differentiation of hDPSCs towards a bone phenotype, as demonstrated by the evaluation of ALP activity. The combination of the two factors lead to a higher effect on ALP expression in comparison with cells treated with only differentiation factors; moreover, also the evaluation of mineralized matrix deposition, performed by Alizarin Red assay, proved the synergic effect of CTL and differentiation stimuli on cell response. The biological relevance of CTL was more appreciable in the

Alg/HAp scaffolds: CTL was able to improve cell adhesion on alginate trabeculae. The ability of Alg/HAp scaffolds to sustain cell adhesion and proliferation has been already reported for MG63 cells (Turco et al., 2009) and hDPSCs (Sancilio et al., 2018), demonstrating that the incorporation of HAp is sufficient to overcome the biological inertness of alginate. The ability of CTL to sustain and improve cell adhesion in alginate structures was already proven for other cell types like chondrocyte (Donati et al., 2005) and neurons (Medelin et al., 2018). Regarding cell proliferation of hDPSCs seeded on the scaffolds, no influence of CTL on this biological process was observed. Considering the higher adhesion of hDPSCs in CTL-sc, the lack of difference between proliferation of hDPSCs in CTL-sc compared to Ctrl-sc, could be attributed to a partial loss of cells due to the initial release of CTL. In light of this, the preparation of CTL-sc needs to be optimized to increase the stability of CTL coating. Moreover, even though the colonization of Alg/HAp and CTL coated scaffolds has been successfully performed under static conditions (Marsich, Bellomo, et al., 2013; Porrelli et al., 2015; Sancilio et al., 2018; Turco et al., 2009), a critical issue related to the cell culture in three-dimensional structures is the achieving of a uniform scaffolds colonization. A limitation of this study is that the static culture conditions here used may not be sufficient to achieve a proper colonization of the scaffolds; therefore, future experiments performed with bioreactors, that allow perfusion of the scaffold with culture media and cells, will be useful to better investigate colonization of the scaffolds by the cells (Allori et al., 2016; Beskardes et al., 2018). The most relevant result was the evaluation of CTL influence on hDPSCs differentiation: indeed, a strong synergistic effect on ALP expression can be observed combining CTL-sc with DS. This effect was significantly higher than the sum of the effects of CTL-sc without DS, or Ctrl-sc with DS, indicating that the three-dimensional structure of the scaffolds provides an environment, which strongly stimulate the growth and differentiation of hDPSCs. The molecular mechanisms by which CTL induces stem cell differentiation towards an osteoblast phenotype are not yet understood. The biological effects of the differentiation stimuli used here are higher than those of CTL alone, which is unable to act directly at the molecular level and to activate the mechanisms triggered by growth factors. The synergistic effect of CTL and DS could be explained by the hypothesis that CTL, thanks to a chemical affinity, is able to increase the local concentration and availability of the differentiation stimuli. Moreover, as CTL is able to interact with Galectins and membrane receptors, it might be able to enhance the biological response of cells to differentiation stimuli by affecting interactions between the cells and the membrane receptors. This phenomenon could be explained considering the so called "cell receptor clustering" (Di Iorio et al., 2020): the clustering of cell receptors upon interaction with multivalent ligands (Grochmal et al., 2013) or with ECM components (Kim et al., 2011) plays a major role in cellular processes and in the cell responses to growth factors. In this context, CTL could be able to act as a multivalent ligand, or in a similar way to ECM glycans, and to trigger a receptor clustering higher responsive to differentiation stimuli. It is worthy of notice that an involvement of Galectin 3 (Priglinger et al., 2013) and Galectin 1 (Rossi et al., 2006) in the receptor clustering process, was observed. Further experiments for the evaluation of the interactions between CTL, galectins and receptors at the molecular level will be necessary to deeply understand these phenomena. The positive influence of a three-dimensional environment on the adhesion, growth and differentiation of hDPSCs has been already widely stressed in the literature: in this context, alginate-based scaffolds and hydrogels proved to support the osteogenic, odontogenic and chondrogenic abilities of hDPSCs (Bhoj et al., 2015; Kanafi et al., 2014; Karadzic et al., 2015; Kumabe et al., 2006; Mata et al., 2017; Umemura et al., 2011). In particular Alg/HAp scaffolds were recently used as an osteoconductive structure able to sustain adhesion, growth and differentiation of hDPSCs, promoting the deposition of extracellular matrix (Sancilio et al., 2018). ALP is, indeed, a marker of early osteoblast differentiation, therefore further experiments evaluating the expression of osteocalcin and osteopontin as well as the molecular mechanisms of cell adhesion on scaffolds, will be performed to better investigate the biological functions of scaffolds and CTL. A major limitation of this study is that the evaluation of the biological properties of scaffolds and of the biological role of CTL was performed in vitro. Therefore, future in vivo experiments, that could be performed on non-critical bone defects of rabbit or minipig models, will be necessary to confirm the in vivo ability of scaffolds to sustain bone formation.

5. Conclusions

Osteoconductive and osteoinductive porous scaffolds were prepared using alginate, hydroxyapatite and a bioactive lactose-modified chitosan (CTL). The structures are stable over time and compatible with cell adhesion and differentiation, and with extracellular matrix deposition. hDPSCs were used as a cell model to evaluate the biological effects of the scaffolds and of CTL. Cell cultures revealed that CTL is able to increase alkaline phosphatase activity and extracellular matrix deposition, in combination with differentiation stimuli. Moreover, when CTL is used as coating for porous scaffolds, cell adhesion is improved and the osteogenic activity increases synergistically when differentiation stimuli are added. Overall, the data showed the ability of CTL to induce the differentiation of hDPSCs towards bone phenotype and the promising potential of CTL-scaffolds that could be used in combination with hDPSCs to hasten bone healing. Further experiments are necessary to deeply investigate the biological role of CTL in terms of cell adhesion and osteoblast differentiation. Moreover, the biological properties related to the scaffold three-dimensional structure and the ability of cells to colonize these structures will be evaluated by means of dynamic culturing conditions.

Funding sources

This research did not receive any specific grant from funding agencies in the public, commercial, or not-for-profit sectors.

CRediT authorship contribution statement

Davide Porrelli: Conceptualization, Investigation, Data curation, Formal analysis, Visualization, Writing – original draft. **Martina Gruppuso:** Investigation, Data curation, Writing – original draft. **Federica Vecchies:** Conceptualization, Investigation, Data curation, Writing – original draft. **Eleonora Marsich:** Conceptualization, Validation, Supervision, Writing – review & editing. **Gianluca Turco:** Conceptualization, Validation, Supervision, Writing – review & editing.

Declaration of competing interest

The authors Gianluca Turco and Eleonora Marsich declare to be a shares holders of the company BiopoLife.

Appendix A. Supplementary data

Stemness characterization of hDPSCs by means of optical microscopy and flow cytometry; evaluation of Galectin-1 expression from hDPSCs. Supplementary data to this article can be found online at https://doi.org/10.1016/j.carbpol.2021.118610.

References

Abhinandan, R., Pranav Adithya, S., Saleth Sidharthan, D., Balagangadharan, K., & Selvamurugan, N. (2021). Synthesis and characterization of magnesium diboride nanosheets in alginate/polyvinyl alcohol scaffolds for bone tissue engineering. *Colloids and Surfaces B: Biointerfaces, 203*, Article 1117711. https://doi.org/10.1016/j.colsurfb.2021.111771

Aghazadeh, M., Samiei, M., Alizadeh, E., Porkar, P., Bakhtiyari, M., & Salehi, R. (2017). Towards osteogenic bioengineering of dental pulp stem induced by sodium fluoride

on hydroxyapatite based biodegradable polymeric scaffold. *Fibers and Polymers, 18*(8), 1468–1477. https://doi.org/10.1007/s12221-017-7120-0
Ahsan, S. M., Thomas, M., Reddy, K. K., Sooraparaju, S. G., Asthana, A., & Bhatnagar, I. (2018). Chitosan as biomaterial in drug delivery and tissue engineering. *International Journal of Biological Macromolecules, 110*, 97–109. https://doi.org/10.1016/j.ijbiomac.2017.08.140
Aimetti, M., Ferrarotti, F., Cricenti, L., Mariani, G., & Romano, F. (2014). Autologous dental pulp stem cells in periodontal regeneration: A case report. *The International Journal of Periodontics & Restorative Dentistry, 34*(Suppl), s27–s33. https://doi.org/10.11607/prd.1635
Aimetti, M., Ferrarotti, F., Gamba, M., Giraudi, M., & Romano, F. (2018). Regenerative treatment of periodontal intrabony defects using autologous dental pulp stem cells: A 1-year follow-up case series. *The International Journal of Periodontics & Restorative Dentistry, 38*(1), 51–58. https://doi.org/10.11607/prd.3425
Akpinar, G., Kasap, M., Aksoy, A., Duruksu, G., Gacar, G., & Karaoz, E. (2014). Phenotypic and proteomic characteristics of human dental pulp derived Mesenchymal Stem Cells from a natal, an exfoliated deciduous, and an impacted third molar tooth. *Stem Cells International, 2014*(19). https://doi.org/10.1155/2014/457059
Albrektsson, T., Chrcanovic, B., Östman, P.-O., & Sennerby, L. (2017). Initial and long-term crestal bone responses to modern dental implants. *Periodontology, 73*(1), 41–50. https://doi.org/10.1111/prd.12176 (2000).
Alkaisi, A., Ismail, A. R., Mutum, S. S., Rifin Ahmad, Z. A., Masudi, S., & Razak, N. H. A. (2013). Transplantation of human Dental Pulp Stem Cells: Enhance bone consolidation in mandibular distraction osteogenesis. *Journal of Oral and Maxillofacial Surgery, 71*(10). https://doi.org/10.1016/j.joms.2013.05.016 (1758. e1–1758.e13).
Allori, A. C., Davidson, E. H., Reformat, D. D., Sailon, A. M., Freeman, J., Vaughan, A., … Warren, S. M. (2016). Design and validation of a dynamic cell-culture system for bone biology research and exogenous tissue-engineering applications. *Journal of Tissue Engineering and Regenerative Medicine, 10*, E327–E336. https://doi.org/10.1002/term1810
Alves, N. M., & Mano, J. F. (2008). Chitosan derivatives obtained by chemical modifications for biomedical and environmental applications. *International Journal of Biological Macromolecules, 43*(5), 401–414. https://doi.org/10.1016/j.ijbiomac.2008.09.007
Amini, A. R., Laurencin, C. T., & Nukavarapu, S. P. (2012). Bone tissue engineering: Recent advances and challenges. *Critical Reviews in Biomedical Engineering, 40*(5), 363–408. https://doi.org/10.1615/CritRevBiomedEng.v40.i5.10
Andersen, H., Jense, O. N., Moiseeva, E. P., & Eriksen, E. (2003). A proteome study of secreted prostatic factors affecting osteoblastic activity: Galectin-1 is involved in differentiation of human Bone Marrow Stromal Cells. *Journal of Oral and Mineral Research, 18*, 195–203. https://doi.org/10.1359/jbmr.2003.18.2.195
Asghari Sana, F., Çapkın Yurtsever, M., Kaynak Bayrak, G., Tunçay, E.Ö., Kiremitçi, A. S., & Gümüşderelioğlu, M. (2017). Spreading, proliferation and differentiation of human dental pulp stem cells on chitosan scaffolds immobilized with RGD or fibronectin. *Cytotechnology, 69*(4), 617–630. https://doi.org/10.1007/s10616-017-0072-9
Barbieri, M., Brizi, L., Bortolotti, V., Fantazzini, P., Nogueira d'Eurydice, M., Obruchkov, S., … Galvosas, P. (2018). Single-sided NMR for the diagnosis of osteoporosis: Diffusion weighted pulse sequences for the estimation of trabecular bone volume fraction in the presence of muscle tissue. *Microporous and Mesoporous Materials, 269*, 166–170. https://doi.org/10.1016/j.micromeso.2017.05.023
Battafarano, G., Rossi, M., De Martino, V., Marampon, F., Borro, L., Secinaro, A., & Del Fattore, A. (2021). Strategies for bone regeneration: From graft to tissue engineering. *International Journal of Molecular Sciences, 22*(3), 1128. https://doi.org/10.3390/ijms22031128
Beskardes, I. G., Aydin, G., Bektas, S., Cengiz, A., & Gümüsderelioglu, M. (2018). A systematic study for optimal cell seeding and culture conditions in a perfusion mode bone-tissue bioreactor. *Biochemical Engineering Journal, 132*, 100–111. https://doi.org/10.1016/j.bej.2018.01.006
Bhoj, M., Zhang, C., & Green, D. (2015). A first step in de novo synthesis of a living pulp tissue replacement using dental pulp MSCs and tissue growth factors, encapsulated within a bioinspired alginate hydrogel. *Journal of Endodontics, 41*(7), 1100–1107. https://doi.org/10.1016/j.joen.2015.03.006
Bianco, P., & Robey, P. G. (2001). Stem cells in tissue engineering. *Nature, 414*(6859), 118–121. https://doi.org/10.1038/35102181
Bosshardt, D. D., Chappuis, V., & Buser, D. (2017). Osseointegration of titanium, titanium alloy and zirconia dental implants: Current knowledge and open questions. *Periodontology, 73*(1), 22–40. https://doi.org/10.1111/prd.12179 (2000).
Bouet, G., Marchat, D., Cruel, M., Malaval, L., & Vico, L. (2015). In vitro three-dimensional bone tissue models: From cells to controlled and dynamic environment. *Tissue Engineering. Part B, Reviews, 21*(1), 133–156. https://doi.org/10.1089/ten.TEB.2013.0682
Camby, I., Le Mercier, M., Lefranc, F., & Kiss, R. (2006). Galectin-1: A small protein with major functions. *Glycobiology, 16*(11), 137R–157R. https://doi.org/10.1093/glycob/cwl025
Cameraro-Espinosa, S., & Moroni, L. (2021). Janus 3D printed dynamic scaffolds for nanovibration-driven bone regeneration. *Nature Communications, 12*, 1031. https://doi.org/10.1038/s41467-021-21325-x
Choi, J. Y., van Wijnen, A. J., Aslam, F., Leszyk, J. D., Stein, J. L., Stein, G. S., … Penman, S. (1998). Developmental association of the beta-galactoside-binding protein galectin-1 with the nuclear matrix of rat calvarial osteoblasts. *Journal of Cell Science, 111*(20), 3035–3043. https://doi.org/10.1242/jcs.111.20.3035
D'Amelio, N., Esteban, C., Coslovi, A., Feruglio, L., Uggeri, F., Villegas, M., … Donati, I. (2013). Insight into the molecular properties of Chitlac, a chitosan derivative for tissue engineering. *The Journal of Physical Chemistry B, 117*(43), 13578–13587. https://doi.org/10.1021/jp4067263
De Santis, R., Gloria, A., Russo, T., D'Amora, U., Zeppetelli, S., Tampieri, A., … Ambrosio, L. (2011). A route toward the development of 3D magnetic scaffolds with tailored mechanical and morphological properties for hard tissue regeneration: Preliminary study. *Virtual and Physical Prototyping, 6*(4), 189–195. https://doi.org/10.1080/17452759.2011.631324
Di Iorio, D., Lu, Y., Meulman, J., & Huskens, J. (2020). Recruitment of receptors at supported lipid bilayers promoted by the multivalent binding of ligand modified unilamellar vesicles. *Chemical Science, 11*, 3307. https://doi.org/10.1039/d0sc00518e
Donati, I., Stredanska, S., Silvestrini, G., Vetere, A., Marcon, P., Marsich, E., Mozetic, P., Gamini, A., Paoletti, S., & Vittur, F. (2005). The aggregation of pig articular chondrocyte and synthesis of extracellular matrix by a lactose-modified chitosan. *Biomaterials, 26*(9), 987–998. https://doi.org/10.1016/j.biomaterials.2004.04.015
Doube, M., Kłosowski, M. M., Arganda-Carreras, I., Cordelières, F. P., Dougherty, R. P., Jackson, J. S., … Shefelbine, S. J. (2010). BoneJ: Free and extensible bone image analysis in ImageJ. *Bone, 47*(6), 1076–1079. https://doi.org/10.1016/j.bone.2010.08.023
Fisher, J. N., Peretti, G. M., & Scotti, C. (2016). Stem cells for bone regeneration: From cell-based therapies to decellularised engineered extracellular matrices. *Stem Cells International, 2016*, 15. https://doi.org/10.1155/2016/9352598
Fradique, R., Correia, T. R., Miguel, S. P., de Sá, K. D., Figueira, D. R., Mendonça, A. G., & Correia, I. J. (2016). Production of new 3D scaffolds for bone tissue regeneration by rapid prototyping. *Journal of Materials Science: Materials in Medicine, 27*(4), 69. https://doi.org/10.1007/s10856-016-5681-x
Furlani, F., Sacco, P., Cok, M., de Marzo, G., Marsich, E., Paoletti, S., & Donati, I. (2019). Biomimetic, multiresponsive, and self-healing lactose-modified chitosan (CTL)-based gels formed via competitor-assisted mechanism. *ACS Biomaterials Science & Engineering, 5*(10), 5539–5547. https://doi.org/10.1021/acsbiomaterials.9b01256
Furlani, F., Sacco, P., Marsich, E., Donati, I., & Paoletti, S. (2017). Highly monodisperse colloidal coacervates based on a bioactive lactose-modified chitosan: From synthesis to characterization. *Carbohydrate Polymers, 174*, 360–368. https://doi.org/10.1016/j.carbpol.2017.06.097
Ghanaati, S., Barbeck, M., Hilbig, U., Hoffmann, C., Unger, R. E., Sader, R. A., … Kirkpatrick, C. J. (2011). An injectable bone substitute composed of beta-tricalcium phosphate granules, methylcellulose and hyaluronic acid inhibits connective tissue influx into its implantation bed in vivo. *Acta Biomaterialia, 7*(11), 4018–4028. https://doi.org/10.1016/j.actbio.2011.07.003
Grasdalen, H. (1983). High-field, 1H-n.m.r. spectroscopy of alginate: Sequential structure and linkage conformations. *Carbohydrate Research, 118*, 255–260. https://doi.org/10.1016/0008-6215(83)88053-7
Grasdalen, H., Larsen, B., & Smidsrød, O. (1979). A p.m.r. Study of the composition and sequence of uronate residues in alginates. *Carbohydrate Research, 68*(1), 23–31. https://doi.org/10.1016/S0008-6215(00)84051-3
Grochmal, A., Ferrero, E., Milanesi, L., & Tomas, S. (2013). Modulation of in-membrane receptor clustering upon binding of multivalent ligands. *Journal of the American Chemical Society, 135*, 10172–10177. https://doi.org/10.1021/ja404428u
Guarino, V., Caputo, T., Altobelli, R., & Ambrosio, L. (2015). Degradation properties and metabolic activity of alginate and chitosan polyelectrolytes for drug delivery and tissue engineering applications. *AIMS Materials Science, 2*(4), 497–502. https://doi.org/10.3934/matersci.2015.4.497
Gupta, A., Woods, M. D., Illingworth, K. D., Niemeier, R., Schafer, I., Cady, C., … El-Amin, S. F., III (2013). Single walled carbon nanotube composites for bone tissue engineering. *Journal of Orthopaedic Research, 31*(9), 1374–1381. https://doi.org/10.1002/jor.22379
Henkel, J., Woodruff, M. A., Epari, D. R., Steck, R., Glatt, V., Dickinson, I. C., … Hutmacher, D. W. (2013). Bone regeneration based on tissue engineering conceptions—A 21st century perspective. *Bone Research, 1*(3), 216–248. https://doi.org/10.4248/BR201303002
Hersel, U., Dahmen, C., & Kessler, H. (2013). RGD modified polymers: Biomaterials for stimulated cell adhesion and beyond. *Biomaterials, 24*(24), 4385–4415. https://doi.org/10.1016/S0142-9612(03)00343-0
Hutmacher, D. W. (2000). Scaffolds in tissue engineering bone and cartilage. *Biomaterials, 21*(24), 2529–2543. https://doi.org/10.1016/S0142-9612(00)00121-6
Kadri, T., Lataillade, J.-J., Doucet, C., Marie, A., Ernou, I., Bourin, P., Joubert-Caron, R., Caron, M., & Lutomski, D. (2005). Proteomic study of Galectin-1 expression in human mesenchymal stem cells. *Stem Cells and Development, 14*(2), 204–212. https://doi.org/10.1089/scd.2005.14.204
Kanafi, M. M., Ramesh, A., Gupta, P. K., & Bhonde, R. R. (2014). Dental pulp stem cells immobilized in alginate microspheres for applications in bone tissue engineering. *International Endodontic Journal, 47*(7), 687–697. https://doi.org/10.1111/iej.12205
Karadzic, I., Vucic, V., Jokanovic, V., Debeljak-Martacic, J., Markovic, D., Petrovic, S., & Glibetic, M. (2015). Effects of novel hydroxyapatite-based 3D biomaterials on proliferation and osteoblastic differentiation of mesenchymal stem cells. *Journal of Biomedical Materials Research Part A, 103*(1), 350–357. https://doi.org/10.1002/jbm.a.35180
Kim, S.-H., Turnbull, J., & Guimond, S. (2011). Extracellular matrix and cell signaling: The dynamic cooperation of integrin, proteoglycan and growth factor receptor. *Journal of Endocrinology, 209*, 139–151. https://doi.org/10.1530/JOE-10-0377
Kokubo, T., Kushitani, H., Sakka, S., Kitsugi, T., & Yamamuro, T. (1990). Solutions able to reproduce in vivo surface-structure changes in bioactive glass-ceramic A-W3. *Journal of Biomedical Materials Research, 24*(6), 721–734. https://doi.org/10.1002/jbm.820240607
Kumabe, S., Nakatsuka, M., Kim, G.-S., Jue, S.-S., Aikawa, F., Shin, J.-W., & Iwai, Y. (2006). Human dental pulp cell culture and cell transplantation with an alginate

scaffold. *Okajimas Folia Anatomica Japonica, 82*(4), 147–155. https://doi.org/10.2535/ofaj.82.147
Li, S., Xiong, Q., Lai, X., Li, X., Wan, M., Zhang, J., Yan, Y., Cao, M., Lu, L., Guan, J., Zhang, D., & Lin, Y. (2016). Molecular modification of polysaccharides and resulting bioactivities. *Comprehensive Reviews in Food Science and Food Safety, 15*(2), 237–250. https://doi.org/10.1111/1541-4337.12161
Li, Z., Ramay, H. R., Hauch, K. D., Xiao, D., & Zhang, M. (2005). Chitosan–alginate hybrid scaffolds for bone tissue engineering. *Biomaterials, 26*(18), 3919–3928. https://doi.org/10.1016/j.biomaterials.2004.09.062
Liu, Q., Sacco, P., Marsich, E., Furlani, F., Arib, C., Djaker, N., de la Chapelle, M., Donati, I., & Spadavecchia, J. (2018). Lactose-modified chitosan gold(III)-PEGylated complex-bioconjugates: From synthesis to interaction with targeted Galectin-1 protein. *Bioconjugate Chemistry, 29*(10), 3352–3361. https://doi.org/10.1021/acs.bioconjchem.8b00520
Ma, L., Yu, Y., Liu, H., Sun, W., Lin, Z., Liu, C., & Miao, L. (2021). Berberine-releasing electrospun scaffold induces osteogenic differentiation of DPSCs and accelerates bone repair. *Scientific Reports, 11*, 1027. https://doi.org/10.1038/s41598-020-79734-9
Mancini, L., Dreossi, D., Fava, C., Sodini, N., Tromba, G., Favretto, S., & Montanari, F. (2007). *TOMOLAB: The new X-ray micro-tomography facility at Elettra.* Elettra Highlights.
Marcon, P., Marsich, E., Vetere, A., Mozetic, P., Campa, C., Donati, I., Vittur, F., Gamini, A., & Paoletti, S. (2005). The role of Galectin-1 in the interaction between chondrocytes and a lactose-modified chitosan. *Biomaterials, 26*(24), 4975–4984. https://doi.org/10.1016/j.biomaterials.2005.01.044
Marsich, E., Bellomo, F., Turco, G., Travan, A., Donati, I., & Paoletti, S. (2013). Nano-composite scaffolds for bone tissue engineering containing silver nanoparticles: Preparation, characterization and biological properties. *Journal of Materials Science: Materials in Medicine, 24*(7), 1799–1807. https://doi.org/10.1007/s10856-013-4923-4
Marsich, E., Travan, A., Donati, I., Turco, G., Kulkova, J., Moritz, N., … Paoletti, S. (2013). Biological responses of silver-coated thermosets: An in vitro and in vivo study. *Acta Biomaterialia, 9*(2), 5088–5099. https://doi.org/10.1016/j.actbio.2012.10.002
Mata, M., Milian, L., Oliver, M., Zurriaga, J., Sancho-Tello, M., Llano, J. J. M.d., & Carda, C. (2017). In vivo articular cartilage regeneration using human Dental Pulp Stem Cells cultured in an alginate scaffold: A preliminary study. *Stem Cells International, 2017*, 9. https://doi.org/10.1155/2017/8309256
Medelin, M., Porrelli, D., Aurand, E. R., Scaini, D., Travan, A., Borgogna, M. A., … Ballerini, L. (2018). Exploiting natural polysaccharides to enhance in vitro bio-constructs of primary neurons and progenitor cells. *Acta Biomaterialia, 73*, 285–301. https://doi.org/10.1016/j.actbio.2018.03.041
Meza, G., Urrejole, D., Saint Jean, N., Inostroza, C., Lopez, V., Khoury, M., & Brizuela, C. (2019). Personalized cell therapy for pulpitis using autologous Dental Pulp Stem Cells and leukocyte platelet-rich fibrin: A case report. *Journal of Endodontics, 45*, 144–149. https://doi.org/10.1016/j.joen.2018.11.009
Misch, C. E., Qu, Z., & Bidez, M. W. (1999). Mechanical properties of trabecular bone in the human mandible: Implications for dental implant treatment planning and surgical placement. *Journal of Oral and Maxillofacial Surgery, 57*(6), 700–706. https://doi.org/10.1016/s0278-2391(99)90437-8
Otsu, N. (1979). A threshold selection method from gray-level histograms. *IEEE Transactions on Systems, Man, and Cybernetics, 9*(1), 62–66. https://doi.org/10.1109/TSMC.1979.4310076
Panzavolta, S., Torricelli, P., Amadori, S., Parrilli, A., Rubini, K., della Bella, E., Fini, M., & Bigi, A. (2013). 3D interconnected porous biomimetic scaffolds: In vitro cell response. *Journal of Biomedical Materials Research Part A, 101*(12), 3560–3570. https://doi.org/10.1002/jbm.a.34662
Park, S.-H., Gil, E. S., Shi, H., Kim, H. J., Lee, K., & Kaplan, D. L. (2010). Relationships between degradability of silk scaffolds and osteogenesis. *Biomaterials, 31*(24), 6162–6172. https://doi.org/10.1016/j.biomaterials.2010.04.028
Podporska-Carroll, J., Ip., J. W. Y., & Gogolewski, S. (2014). Biodegradable poly(ester urethane)urea scaffolds for tissue engineering: Interaction with osteoblast-like MG-63 cells. *Acta Biomaterialia, 10*, 2781–2791. https://doi.org/10.1016/j.actbio.2014.02.016
Porrelli, D., Travan, A., Turco, G., Marsich, E., Borgogna, M., Paoletti, S., & Donati, I. (2015). Alginate-hydroxyapatite bone scaffolds with isotropic or anisotropic pore structure: Material properties and biological behavior. *Macromolecular Materials and Engineering, 30*(10), 989–1000. https://doi.org/10.1002/mame.201500055
Priglinger, C. S., Szober, C. M., Priglinger, S. G., Merl, J., Euler, K. N., Kernt, M., … Hauck, S. M. (2013). Galectin-3 induces clustering of CD147 and Integrin-b1 transmembrane glycoprotein receptors on the RPE cell surface. *PLoS ONE, 8*(7), Article e70011. https://doi.org/10.1371/journal.pone.0070011
Rapino, M., Di Valerio, V., Zara, S., Gallorini, M., Marconi, G. D., Sancilio, S., … Cataldi, A. (2019). Chitlac-coated thermosets enhance osteogenesis and angiogenesis in a co-culture of dental pulp stem cells and endothelial cells. *Nanomaterials, 9*, 928. https://doi.org/10.3390/nano9070928
Roseti, L., Parisi, V., Petretta, M., Cavallo, C., Desando, G., Bartolotti, I., & Grigolo, B. (2017). Scaffolds for bone tissue engineering: State of the art and new perspectives. *Materials Science and Engineering: C, 78*, 1246–1262. https://doi.org/10.1016/j.msec.2017.05.017
Rossi, B., Espeli, M., Schiff, C., & Gauthier, L. (2006). Clustering of pre-B cell integrins induces Galectin-1 dependent pre-B cell receptor relocalization and activation. *The Journal of Immunology, 177*, 796–803. https://doi.org/10.4049/jimmunol.177.2.796
Russo, T., Peluso, V., Gloria, A., Olivieiro, O., Rinaldi, L., Improta, G., … D'Antò, V. (2020). Combination design of time-dependent magnetic field and magnetic nanocomposites to guide cell behavior. *Nanomaterials, 10*, 577. https://doi.org/10.3390/nano10030577
Sancilio, S., Gallorini, M., Di Nisio, C., Marsich, E., Di Pietro, R., Schweikl, H., & Cataldi, A. (2018). Alginate/hydroxyapatite-based nanocomposite scaffolds for bone tissue engineering improve dental pulp biomineralization and differentiation. *Stem Cells International, 2018*, 13. https://doi.org/10.1155/2018/9643721
Schindelin, J., Arganda-Carreras, I., Frise, E., Kaynig, V., Longair, M., Pietzsch, T., … Cardona, A. (2012). Fiji: An open-source platform for biological-image analysis. *Nature Methods, 9*(7), 676–682. https://doi.org/10.1038/nmeth.2019
Sharma, C., Dinda, A. K., Potdar, P. D., Chou, C.-F., & Mishra, N. C. (2016). Fabrication and characterization of novel nano-biocomposite scaffold of chitosan–gelatin–alginate–hydroxyapatite for bone tissue engineering. *Materials Science and Engineering: C, 64*, 416–427. https://doi.org/10.1016/j.msec.2016.03.060
Tatullo, M., Marrelli, M., Shakesheff, K. M., & White, L. J. (2015). Dental pulp stem cells: Function, isolation and applications in regenerative medicine. *Journal of Tissue Engineering and Regenerative Medicine, 9*(11), 1205–1216. https://doi.org/10.1002/term.1899
Tazhitdinova, R., & Timoshenko, A. V. (2020). The emerging role of Galectins and *O*-GlcNAc homeostasis in processes of cellular differentiation. *Cells, 9*, 1792. https://doi.org/10.3390/cells9081792
Tettamanti, L., Andreasi Bassi, M., Trapella, G., Candotto, V., & Tagliabue, A. (2017). Applications of biomaterials for bone augmentation of jaws: Clinical outcomes and in vitro studies. *Oral Implantology, 10*(1), 37–44. https://doi.org/10.11138/orl/2017
Turco, G., Marsich, E., Bellomo, F., Semeraro, S., Donati, I., Brun, F., Grandolfo, M., Accardo, A., & Paoletti, S. (2009). Alginate/hydroxyapatite biocomposite for bone ingrowth: A trabecular structure with high and isotropic connectivity. *Biomacromolecules, 10*(6), 1575–1583. https://doi.org/10.1021/bm900154b
Turco, G., Porrelli, D., Marsich, E., Vecchies, F., Lombardi, T., Stacchi, C., & Di Lenarda, R. (2018). Three dimensional bone substitutes for oral and maxillofacial surgery: Biological and structural characterization. *Journal of Functional Biomaterials, 9*(4), 62. https://doi.org/10.3390/jfb9040062
Umemura, E., Yamada, Y., Nakamura, S., Ito, K., Hara, K., & Ueda, M. (2011). Viable cryopreserving tissue-engineered cell-biomaterial for cell banking therapy in an effective cryoprotectant. *Tissue Engineering Part C: Methods, 17*(8), 799–807. https://doi.org/10.1089/ten.tec.2011.0003
Urist, M. R. (1965). Bone: Formation by autoinduction. *Science, 150*(3698), 893–899. https://doi.org/10.1126/science.150.3698.893
Vold, I. M. N., Kristiansen, K. A., & Christensen, B. E. (2006). A study of the chain stiffness and extension of alginates, in vitro epimerized alginates, and periodate-oxidized alginates using size-exclusion chromatography combined with light scattering and viscosity detectors. *Biomacromolecules, 7*(7), 2136–2146. https://doi.org/10.1021/bm060099n
Wahl, D. A., & Czernuszka, J. T. (2006). Collagen-hydroxyapatite composites for hard tissue repair. *European Cells & Materials, 11*, 43–56. https://doi.org/10.22203/ecm.v011a06
Yasmeen, S., Lo, M. K., Bajracharya, S., & Roldo, M. (2014). Injectable scaffolds for bone regeneration. *Langmuir, 30*(43), 12977–12985. https://doi.org/10.1021/la503057w
Zhang, D., Wu, X., Chen, J., & Lin, K. (2018). The development of collagen based composite scaffolds for bone regeneration. *Bioactive Materials, 3*(1), 129–138. https://doi.org/10.1016/j.bioactmat.2017.08.004
Zhao, R., Yang, R., Cooper, P. R., Khurshid, Z., Shavandi, A., & Ratnayake, J. (2021). Bone grafts and substitutes in dentistry: A review of current trends and developments. *Molecules, 26*(19), 3007. https://doi.org/10.3390/molecules26103007